THE JOURNAL OF PHYSICAL CHEMISTRY Letters

Letter

pubs.acs.org/JPCL

Inhomogeneity in Ethylammonium Nitrate−Acetonitrile Binary Mixtures: The Highest "Low *q* Excess" Reported to Date

Alessandro Mariani,*[,⊥,†] Ruggero Caminiti,[†,‡] Fabio Ramondo,[§] Giovanna Salvitti,[§] Francesca Mocci,[∥] and Lorenzo Gontrani*[,†]

[†]Dipartimento di Chimica, La Sapienza Università di Roma, Piazzale Aldo Moro 5, 00185 Rome, Italy

[‡]Centro di Ricerca per le Nanotecnologie Applicate all'Ingegneria, Laboratorio per le Nanotecnologie e le Nanoscienze, La Sapienza Università di Roma, Piazzale Aldo Moro 5, 00185 Rome, Italy

[§]Dipartimento di Scienze Fisiche e Chimiche, Università degli Studi dell'Aquila, Via Vetoio, L'Aquila I-67100, Italy

[∥]Dipartimento di Scienze Chimiche e Geologiche, Università di Cagliari, S.S. 554 Km 4,500, I-09042 Monserrato, Italy

Supporting Information

ABSTRACT: The binary mixtures of the ionic liquid ethylammonium nitrate with acetonitrile have been studied by means of wide- and small-angle X-ray scattering and via two different computational methods, namely, classical molecular dynamics and DFT. The recently debated odd feature in the extreme low *q* region of some ionic liquid-based binary mixtures is linked to density fluctuations within the system. We show how the "low *q* excess" is due to some nanoscopic objects which are formed at certain compositions. These structures have different density with respect to the surrounding, thus generating the feature observed. Our results also show how the local arrangement is directly linked to the long-range structure. Moreover, we found once again a similarity in the physicochemical behavior of ethylammonium nitrate and water.

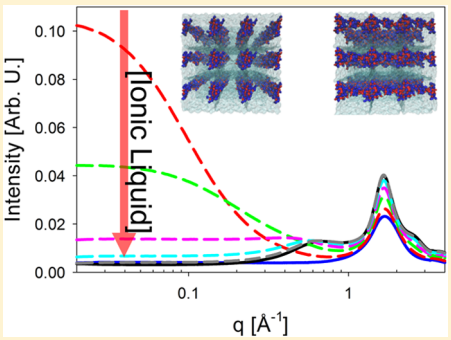

Dissolving a cosolvent into an ionic liquid (IL) may have a variety of effects depending on the nature of the salt and on the added compound.[1−3] Taking ethylammonium nitrate (EAN) as a prototype, there is a wide range of literature concerning the effects that mixing has on its structure.[4−19] The molecular arrangement of neat EAN (Figure 1) is shared with a

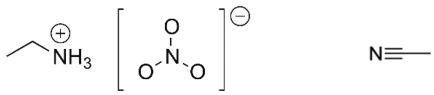

Figure 1. Schematic representation of (left) ethylammonium nitrate and (right) acetonitrile.

number of other ILs and consists of a nanosegregation of two domains (polar and apolar) percolating each other.[8,20,21] This is the so-called sponge-like structure that is responsible for the low *q* peak (LqP) in the small-angle X-ray scattering (SAXS) patterns of these compounds.[22,23] Recently it has been reported that the addition of *n*-alcohols to some ILs leads to an unexpected feature in the extreme low-*q* region of the SAXS pattern, which is termed "low *q* excess" (LqE).[24,25] Greaves and Drummond observed that in some EAN−alcohol mixtures, some micellar-like structures could be found.[26] A confirmation of this behavior came from Jiang et al. stating that when the alcohol alkyl chain is longer than twice that of the IL, then it is too big to be accommodated into the apolar domain, thus forming a series of self-assembled structures where the cation acts as a cosurfactant.[25] In fact, they report the LqE for a variety of systems and always when the ratio between the chain lengths of the IL and the alcohol is less than 0.5. Nevertheless, this interpretation cannot explain why the same effect is found in EAN−methanol mixtures,[24] where one may expect a total mutual miscibility, because methanol is small enough to fit easily in EAN apolar domain. For that system, when LqE was first observed by Russina et al., an explanation in terms of ionic liquid molecules clustering was proposed to explain that odd feature: their empirical potential structure refinement (EPSR) (reverse Monte Carlo) simulations suggested that the feature below 0.3 Å^{-1} was generated by EAN clusters floating into a methanol *sea*. While the structure factor obtained by EPSR finely reproduced the experimental data, such a rigid interpretation is unlikely to be invoked for a liquid, macroscopically homogeneous phase. More recent findings, on EAN−1-pentanol systems,[17] suggest that the origin of the LqE is a more complex critical phenomenon related to the density and concentration fluctuations experienced by the system at its incipient demixing. We have pointed out that the LqE is much more common than one may believe, and it is not limited to protic ionic liquid−*n*-alcohol systems. In our previous work,[18] the LqE was reported for EAN−1,2-dimethoxyethane and EAN−1,4-diaminobutane, both symmet-

Received: May 18, 2017
Accepted: June 26, 2017
Published: June 26, 2017

DOI: 10.1021/acs.jpclett.7b01244
J. Phys. Chem. Lett. 2017, 8, 3512−3522

ric (nonamphiphilic) compounds. Our analysis suggested that the key quantity that may be directly linked to the LqE is the enthalpy of mixing. More precisely, an ionic liquid−molecular compound binary mixture will show the LqE when the enthalpy of mixing of the two components is larger than 30 kJ/mol for that composition. On the basis of our findings, the cause behind this unexpected feature in the SAXS patterns of some systems may be related to an incipient demixing of the sample driven by the lack of molecular affinity between the IL and the cosolvent. Thus, LqE is linked to incipient structural transition of the system. Classical molecular dynamics (MD) is the state-of -the-art technique to interpret, predict, and understand complex systems, and it is widely used when ILs are considered.[3,27,28] Its limitation in neglecting electronic effects is overcome by the chance to simulate large systems, up to several thousand atoms, a task that would be impossible for ab initio calculations. Nevertheless, good results have been achieved with MD in the field of ionic liquids, also when LqE is involved, as in our previous work. DFT calculations of small clusters can give a much more reliable insight on the local short-range molecular arrangement than the picture given from MD. For this reason, we have considered also some small ab initio models.

In the present Letter, we show how acetonitrile (ACN) interacts with EAN when they are mixed together. ACN is structurally similar to methanol, but it is unable to donate hydrogen bonds; therefore, it is the perfect candidate to check if the hydrogen bond has a role in the LqE observation. Density fluctuations have been reported for aqueous mixtures of acetonitrile,[29−33] for which various groups have pointed out how water and acetonitrile do not homogeneously mix but rather organize themselves into water-rich and acetonitrile-rich regions percolating each other. For this system, the LqE is also observed, and it was analyzed in terms of concentration fluctuation parameters, Kirkwood−Buff integrals (KBIs)[34] and/or Ornstein−Zernike (OZ) formalism. Each approach may take advantage of a range of computational techniques to get an atomistic insight into the structure. Nishikawa et al.[29] used concentration fluctuation parameters and KBIs to interpret their SAXS data. Basing their rationalization on the work of Koga et al.,[35] they stated that the acetonitrile−water mixture is made of large clusters of the pure compounds, without trace of an extended hydrogen bond network, unlike the homologous water−methanol system. Subsequent studies involving several experimental and computational methods confirmed this picture that is now firmly supported. In this work, we present the molecular arrangement of EAN−ACN mixtures. We will interpret the experimental SAXS data using OZ formalism, then we will propose a computational model obtained by classical MD simulations. Finally, we will propose some small ab initio models to highlight the short-range molecular arrangement. Our observations are completely in line with those of Perron et al.[36] who studied EAN−acetonitrile binary mixtures as a model for highly concentrated electrolyte solutions. The SAXS patterns collected as a function of composition are plotted in Figure 2.

It is evident how at low EAN concentrations, in the extreme low-q region the scattered intensity has a very high and broad feature. Like all the previously reported systems, the LqE has its maximum intensity at the lower (analyzed) EAN concentration,[17,18,24,25] and here we present the highest LqE ever observed for this kind of system. Although MD models are not large enough (100 Å box side) to properly describe the range with q smaller than 0.15 Å^{-1}, the curves show a markedly steep

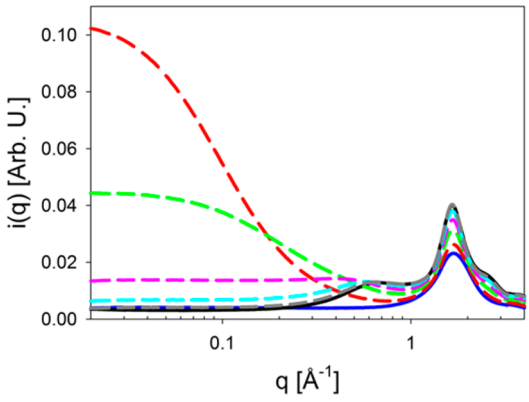

Figure 2. Small- and wide-angle X-ray scattering patterns of the systems studied. χ_{EAN} 0 (blue); 0.1 (red); 0.3 (green); 0.5 (purple); 0.7 (cyan); 0.9 (gray); 1 (black).

rise approaching the lower q limit (see the Supporting Information), and as demonstrated elsewhere,[18] the initial slope of the LqE is reproduced by the models. The OZ formalism describes the diffracted intensity $i(q)$, expressed in arbitrary units, as

$$i(q) = \frac{i(0)}{1 + \xi^2 q^2} + \mathrm{bg} \tag{1}$$

where ξ is the correlation length of electron density fluctuations, bg the background contribution, and $i(0)$ the scattered intensity at $q = 0$, in turn expressed in arbitrary units. To obtain the structure factor $I(q)$ in absolute units, one must normalize $i(q)$ using the formula

$$I(q) = i(q) - \sum x_i f_i^2 \tag{2}$$

where x_i and f_i are the numerical concentration and the scattering factor of atom i, respectively. $I(0)$ is related to the isothermal compressibility κ_T by

$$I(0) = \rho_N k_B T \kappa_T \tag{3}$$

where k_B is the Boltzmann constant, T the temperature in Kelvin, and ρ_N the number density of the system obtained by

$$\rho_N = \frac{N_A \cdot \rho}{\chi_{EAN} \cdot \mathrm{MW}_{EAN} + (1 - \chi_{EAN}) \cdot \mathrm{MW}_{Acetonitrile}} \tag{4}$$

where N_A is Avogadro's number and ρ is the mass density of the system; χ represents the molar fraction, and MW is the molecular weight.

When eq 3 is applied to compute the acetonitrile κ_T, a value of 1150 TPa^{-1} was found, in excellent agreement with 1154 TPa^{-1} reported by Grant-Taylor and Macdonald,[37] confirming the quality of the procedure and the data. In our case, the scattered intensity is much higher than the background, so the latter is negligible. Fitting the lowest-q region of the experimental data with an OZ-like function, one is able to retrieve both $i(0)$ and ξ. Another way to estimate $i(0)$ comes from the Ornstein−Zernike plot. When the reciprocal of the scattered intensity is plotted as a function of q^2, a linear relationship is observed, which makes easier the extrapolation to $q = 0$. The results of both the approaches are shown in Figure 3a, and the fitting parameters for eq 1 are reported in Figure 3b together with κ_T obtained by applying eq 3; Table 1 summarizes the results.

DOI: 10.1021/acs.jpclett.7b01244
J. Phys. Chem. Lett. 2017, 8, 3512−3522

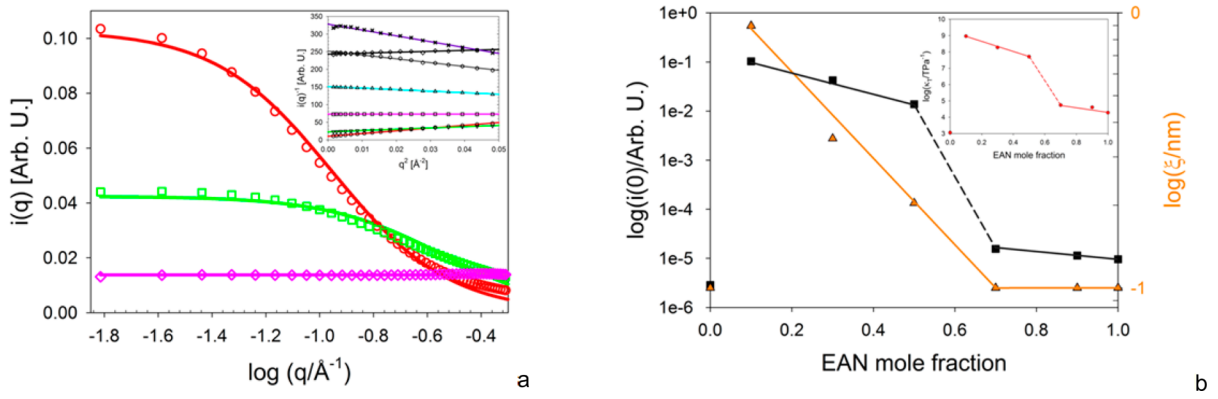

Figure 3. (a) Fitting of the SAXS pattern by an Ornstein−Zernike equation. An Ornstein−Zernike plot is in the inset. The colors are the same as those in Figure 2; experimental data (symbols) and fitting (lines). (b) In the main plot, fitting parameters of the Ornstein−Zernike equation. $i(0)$ (black squares, left-hand y-axis); ξ (orange triangles, right-hand y-axis). Isothermal compressibility of the systems is shown in the inset. Lines are a guide to the eye.

Table 1. Overview of Some Properties of the Systems at 25 °C

χ_{EAN}	$i(0)^a$ [A.U.]	ξ^a [nm]	$\rho_N{}^b$ [molecules·Å^{-3}]	ρ [g·cm^{-3}]	$\kappa_T{}^c$ [TPa^{-1}]
0.00	2.86×10^{-6}	0.1002	0.0468	0.77590	1.15×10^{3}
0.10	1.03×10^{-1}	0.8978	0.0108	0.85719	9.23×10^{8}
0.31	4.24×10^{-2}	0.3496	0.0096	0.98347	1.88×10^{8}
0.50	1.38×10^{-2}	0.2035	0.0086	1.07155	5.17×10^{7}
0.71	1.56×10^{-5}	0.1002	0.0077	1.13984	5.57×10^{4}
0.90	1.14×10^{-5}	0.1001	0.0070	1.18966	4.08×10^{4}
1.00	9.58×10^{-6}	0.1001	0.0122	1.20920	1.91×10^{4}

[a]From eq 1. [b]From eq 4. [c]From eq 3.

Both fitting parameters for eq 1 clearly show two different trend regimes: $i(0)$ steeply increases passing from neat acetonitrile to χ_{EAN} 0.1 and then linearly (in logarithmic scale) decreases as EAN is added to the mixture until a marked step between χ_{EAN} 0.5 and 0.7 breaks the linearity. Starting from χ_{EAN} 0.7, another linear correlation is found, but $i(0)$ has decreased by several orders of magnitude. The step separates the systems showing the LqE ($\chi_{EAN} \leq 0.5$) from the ones which do not do so ($\chi_{EAN} \geq 0.7$). Although the variation in ξ does not show a step, two distinct linear regions are easily individuated. Once again these regions can be linked to the presence or absence of LqE. Here it appears clear that the *objects* responsible for the slope in the extreme low-q region are rapidly formed as the IL is added to acetonitrile with a maximum dimension of ∼0.9 nm at χ_{EAN} 0.1 and then exponentially decrease their size until χ_{EAN} 0.7, where the *objects* associated with the slope are molecular-sized and cannot (obviously) get smaller. A simple, yet powerful way to check the molecular interactions in a binary mixture is the study of the excess molar volume (V^{EX}). This quantity is readily obtained from the experimental density measurements via

$$V^{EX} = \frac{\chi_1 MW_1 + \chi_2 MW_2}{\rho_{exp}} - \left(\frac{\chi_1 MW_1}{\rho_1} + \frac{\chi_2 MW_2}{\rho_2}\right) \quad (5)$$

where MW_x is the molecular weight of component 1 or 2, ρ_{exp} the experimental density, and ρ_x the density of pure 1 or 2. The points obtained were then fitted using a Redlich−Kister function,[38] and the results are shown in Figure 4. The values of V^{EX} for each temperature can be found in Table S1 in the Supporting Information along with experimental densities. Fitting parameters are in Table S2.

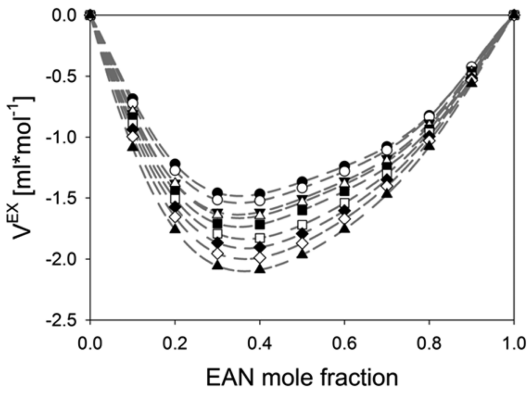

Figure 4. Excess molar volume for ethylammonium nitrate−acetonitrile mixtures: 288 K (●); 293 K (○); 298 K (▼); 303 K (△); 308 K (■); 313 K (□); 318 K (◆); 323 K (◇); 328 K (▲). Data are fitted with a Redlich−Kister function (dashed lines).

V^{EX} values are dependent on two different phenomena, namely, molecular affinity and packing efficiency. In this case, the excess molar volume appears to be negative in the whole composition range for all the considered temperatures, meaning an overall favorable interaction between EAN and ACN, due to one or both the cited effects. When the temperature is varied, the position of the minimum remains almost constant at χ_{EAN} ∼ 0.35, suggesting that on average two hydrogen bond donors on the cation are involved in interactions with as many acetonitrile molecules. Interestingly, when the temperature is increased, all the systems deviate more from ideality, thus enhancing the favorable interactions. It is known that Coulombic forces and hydrogen bonds are weakened upon temperature rising; thus, the stronger interaction must be due to increased packing

DOI: 10.1021/acs.jpclett.7b01244
J. Phys. Chem. Lett. 2017, 8, 3512−3522

efficiency. We have also computed the partial molar volumes differentiating the fitted excess molar volume values for each temperature. The results are reported in Figure 5 and Table S1.

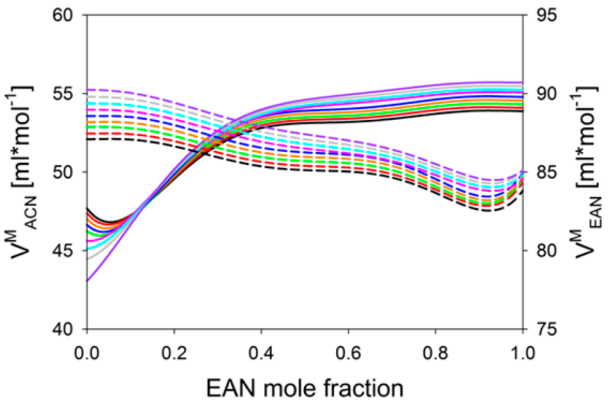

Figure 5. Partial molar volumes for ethylammonium nitrate−acetonitrile mixtures. 288 K (black); 293 K (red); 298 K (green); 303 K (orange); 308 K (blue); 313 K (purple); 318 K (cyan); 323 K (gray); 328 K (violet). EAN (solid line, right-hand *y*-axis); ACN (dashed line, left-hand *y*-axis).

There are four distinct regions in both EAN and ACN partial molar volumes (V^M_{EAN} and V^M_{ACN}, respectively). The first one spans the region $0 < \chi_{EAN} < 0.15$. Here, V^M_{ACN} remains almost constant upon EAN addition, within the studied temperature range. This means that small amounts of IL do not affect the acetonitrile solvation shell; thus, the excluded volume of a single ACN molecule remains constant. On the other hand, V^M_{EAN} shows a distinct minimum at $\chi_{EAN} \sim 0.08$ at 15 °C, which is gradually shifted to the left when the temperature is raised to 40 °C. On further heating, the minimum disappears. It is not common to observe a similar feature in partial molar volume. A system that shows this trend is water−ethanol,[39] for which the minimum appears for the partial molar volume of the alcohol at $\chi_{water} \sim 0.08$. The minimum is due to denser packing of water around the hydrocarbon tail, resulting in an initial decrease of the partial molar volume due to smaller excluded volume of the alcohol molecules. Up to a certain ethanol concentration, all the water molecules will be in the alcohol hydration shell (minimum); upon further addition of ethanol, the effect will be a simple dilution and the partial molar volume will rise. We here suggest a different interpretation based on our other results. Adding small amounts of EAN to acetonitrile, the former does not homogeneously dissolve into the solvent, but it remains self-associated and floats in ACN. This arrangement induces a smaller excluded volume in EAN and consequent smaller number of IL molecules at the acetonitrile interface, suggesting a solvophobic effect. These EAN-rich regions are continuously enlarged on IL addition, until there are too many EAN molecules to be accommodated (minimum), similarly to the effect of water addition to protic ILs reported by Hayes et al.[40] They show how up to a certain water content, the latter can be accommodated into the polar domain of the IL. On further dilution, though, the spongelike structure is destroyed. On further addition, V^M_{EAN} starts to increase as expected. The minimum does not appear at higher temperatures because the system is much more homogeneous. The second region is in the range $0.15 < \chi_{EAN} < 0.45$. Here, V^M_{ACN} regularly decreases on EAN addition; this is because of the estabilizhment of IL−acetonitrile interactions, such as hydrogen bonds, which results is smaller excluded volume of ACN molecules. V^M_{EAN}, instead, steeply increases as EAN is added to the system, suggesting a quick reorganization of the molecular arrangement, consisting in a *relaxation* toward the structure of neat EAN. A third region is in the $0.45 < \chi_{EAN} < 0.8$ range. V^M_{ACN} shows a trend that depends on the temperature. From 15 to 40 °C, V^M_{ACN} remains constant upon EAN addition, and its value is almost equal to the molar volume of neat acetonitrile. This suggest that in this composition range, EAN is unable to sensibly affect the acetonitrile environment. For higher temperatures, the trend is the same of the previous region. On the other hand, V^M_{EAN} still increases but with a much smaller rate with respect to the previous region. This is consistent with the observation on V^M_{ACN} because if EAN "leaves alone" acetonitrile, the reverse is also true. Nevertheless, the presence of a dipolar cosolvent induces some small rearrangement in the IL arrangement. Finally, the fourth region is $\chi_{EAN} > 0.8$. The partial molar volume of EAN remains constant at the value of molar volume of the neat IL. This means that small amounts of acetonitrile do not affect the EAN environment in this region. Interestingly, V^M_{ACN} shows here a minimum. This may suggest the formation of some supramolecular self-assembled structure. Both the results on excess molar volumes and partial molar volumes are finely consistent with the literature. To further understand the temperature effect on the molecular arrangement, the isobaric thermal expansivity α along with its excess values α^{EX} are two powerful tools. We obtained these quantities for system *i* by

$$\alpha_i = \frac{-1}{\rho_i}\left(\frac{\partial \rho_i}{\partial T}\right)_P \tag{6}$$

$$\alpha_i^{EX} = \alpha_i - (\chi_1\alpha_1 + \chi_2\alpha_2) \tag{7}$$

where T is the temperature in Kelvin and P is the pressure. Results are summarized in Figure 6.

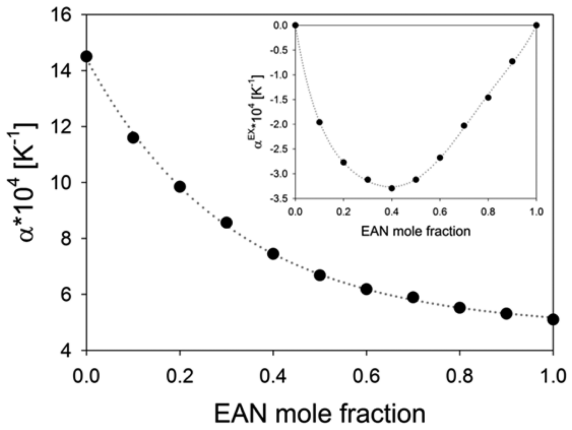

Figure 6. Thermal expansivity for ethylammonium nitrate−acetonitrile mixtures. The inset shows the corresponding excess quantity. Experimental data (points); fit (dotted line).

The expansivity data were fitted using a three-parameter exponential decay function. As can be seen in Figure 6, the agreement is excellent, so adding EAN to the system, α decreases exponentially to the value of neat IL. This can be explained considering that while in neat acetonitrile the molecules are bonded together by only dipole−dipole interaction, the presence of EAN results in the formation of hydrogen bonds and introduces Coulombic forces. Being both

DOI: 10.1021/acs.jpclett.7b01244
J. Phys. Chem. Lett. 2017, 8, 3512−3522

much more persistent with respect to temperature variations than dipole−dipole interactions, the mixture exhibits smaller volume variation upon heating and cooling of the system. The respective excess quantity was fitted using a Redlich−Kister function. It shows negative values for the whole composition range, with a marked minimum at ∼0.4 EAN molar fraction, which somehow corresponds to the threshold between systems that exhibit LqE (χ_{EAN} < ∼0.5) and those that do not. The minimum position is in line with other results on IL−molecular liquid binary systems,[41,42] in which it is shown that aprotic solvents are able to extensively affect the hydrogen bond network, resulting in a minimum in α^{EX} which qualitatively describes the status of the molecular mixing. If the minimum is in the region χ_{IL} < 0.5, then the molecular interactions IL:IL and molecular liquid:molecular liquid are slightly affected by mixing, otherwise the interaction IL:molecular liquid is strong enough to deeply change the molecular organization. In this work the minimum at 0.4 EAN molar fraction suggests that the systems are not homogeneous on a molecular scale. As previously proposed,[17] and similarly to water−acetonitrile,[29] we have associated the *objects* that are responsible for LqE with a density fluctuation. A method that relates the X-ray scattering intensity at $q = 0$ and the fluctuations was formulated by Bhatia and Thornton.[43] The density fluctuation is presented by $\langle(\Delta N)^2\rangle/\bar{N}$, where N is the number of particles in the scattering volume. The angular brackets and lines above letters indicate the average. The relation between the zero-angle intensity, $I(0)$, and concentration fluctuation, $\bar{N}\langle(\Delta c)^2\rangle$, is given by

$$\frac{I(0)}{\bar{N}} = \bar{Z}^2\rho_N k_B T\kappa_T + [\bar{Z}\delta - (Z_{EAN} - Z_{ACN})]^2\bar{N}\langle(\Delta c)^2\rangle \quad (8)$$

where Z is the number of electrons in a molecule and $\bar{Z}$ is

$$\bar{Z} = \chi_{EAN}Z_{EAN} + \chi_{ACN}Z_{ACN} \quad (9)$$

while δ, which considers the difference between the sizes of the cosolvents molecules, has the form

$$\delta = \rho_N(V^M_{EAN} - V^M_{ACN}) \quad (10)$$

The concentration and density fluctuations are related by

$$\frac{\langle(\Delta N)^2\rangle}{\bar{N}} = \rho_N k_B T\kappa_T + \delta^2\bar{N}\langle(\Delta c)^2\rangle \quad (11)$$

The corresponding results are plotted in Figure 7.

It is evident how strong density fluctuations are found at χ_{EAN} 0.1 and then exponentially decrease increasing the IL content in the system. Such important fluctuations are often related to incipient phase separation of the system. We observed no evidence of demixing on mesoscopic scale upon changes of both composition and temperature. Nevertheless, a critical phase separation is possible. There are two kind of such processes, upper critical solution temperature (UCST) and lower critical solution temperature (LCST). The former occurs when demixing takes place, cooling the system; the latter (much less common) refers to phase separation upon heating. To check which one can be associated with EAN−acetonitrile system, we collected the SAXS pattern for χ_{EAN} 0.1 at 40 °C, as reported in Figure 8. The LqE is decreased by temperature rising, thus suggesting an enhanced mixing of the system, meaning that UCST-type is adequate to describe the studied system. This is in line with the results obtained for water−acetonitrile binary mixtures, confirming once more the similarity that water and EAN often show in several physical and chemical properties.

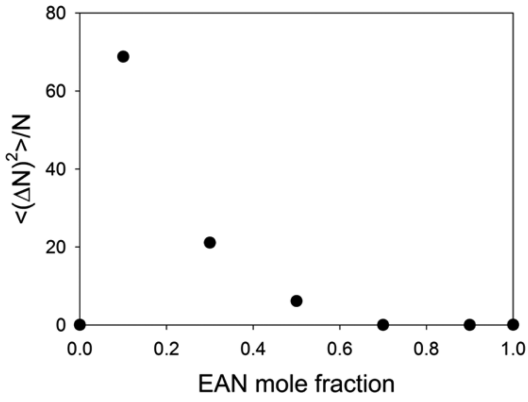

Figure 7. Density fluctuations for ethylammonium nitrate−acetonitrile mixtures.

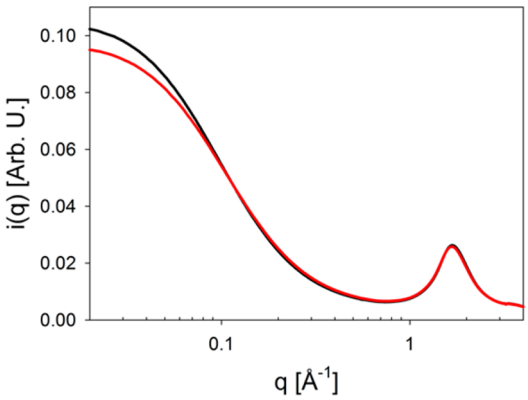

Figure 8. SWAXS patterns for χ_{EAN} 0.1 system at 298 K (black) and 313 K (red).

To understand this system at a molecular level, we took advantage of two different types of computational techniques. From classical MD calculations, we extracted *large-scale* information, while high-resolution details of molecular interactions were probed by DFT. To finely reproduce the LqE, a box with an edge of 130 nm is necessary. This is well beyond the computational power of currently available computers; therefore, we have simulated systems with a side of ∼100 Å, being aware that this allow us to get information down to ∼0.12 Å^{-1}. Nevertheless, we are confident of the reliability of our results, as shown by some of us for other systems in which LqE plays an important role.[18] The quality of our simulations was checked by comparing the experimental wide-angle X-ray scattering (WAXS) patterns and mass densities with the corresponding computed ones. Such comparisons are shown in Figure S1 and Table S1. The snapshots of the simulation boxes are shown in Figure 9; at χ_{EAN} 0.1, we report the central box (PBC unit cell) together with two periodic images on each x, y, and z axes, summing to a box 27 times the minimum image.

We are aware that a simple geometric copy of the simulation box in space is far from being equivalent to a simulation of a larger system, but Figure 9a,a′ has the advantage of giving the clear idea of how inhomogeneous the χ_{EAN} 0.1 mixture is. There, wormlike structures made up of EAN are floating in an acetonitrile sea; of course the real organization is much less

DOI: 10.1021/acs.jpclett.7b01244
J. Phys. Chem. Lett. 2017, 8, 3512−3522

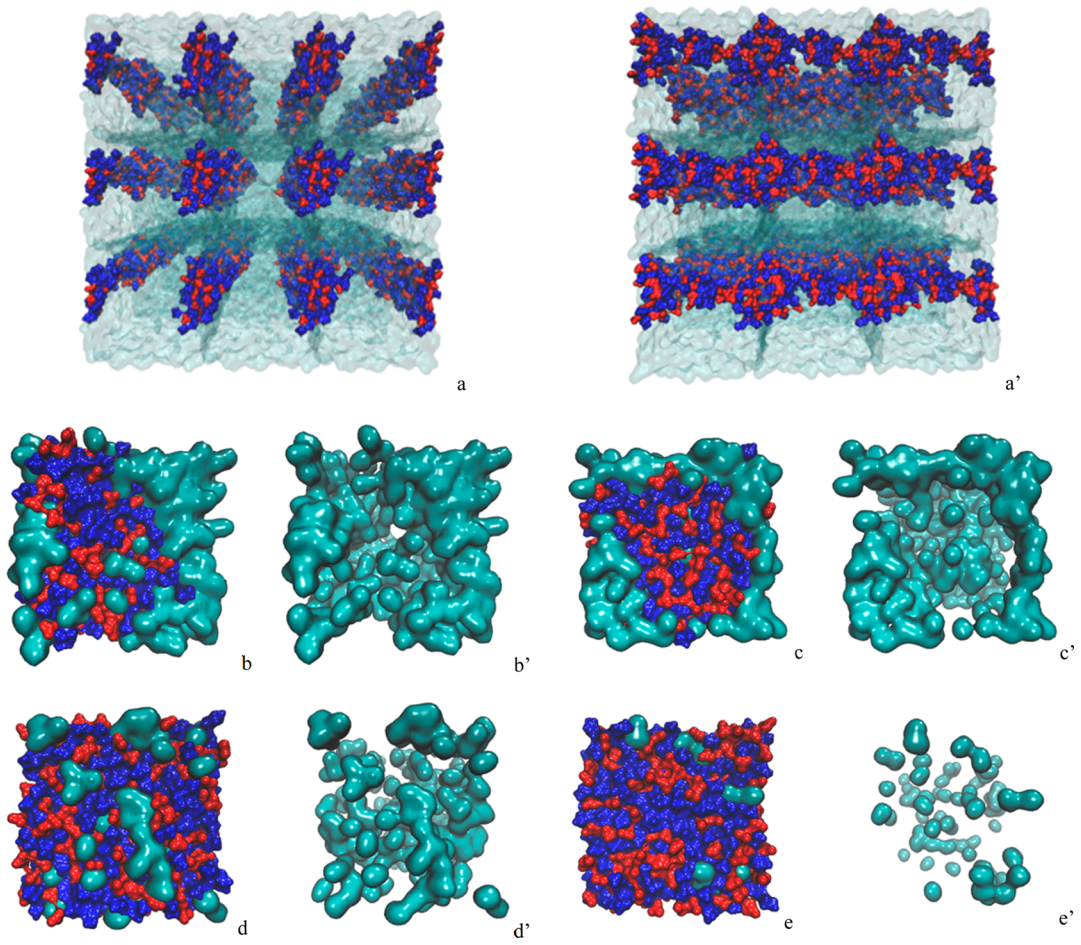

Figure 9. Snapshots of the simulation boxes of ethylammonium nitrate−acetonitrile mixtures. (a, a′) two different views for χ_{EAN} 0.1 system. For all the other systems, plain letters mean that all the molecules are shown, while primed letters mean that just acetonitrile molecules are shown: (b) χ_{EAN} 0.3; (c) 0.5; (d) 0.7; (e) 0.9. Cation (blue); anion (red); acetonitrile (cyan).

ordered, but we are confident that similar structures can be found in that mixture and that they are responsible for the density fluctuations and, therefore, for the LqE. In fact, the decay slope of the $I(q)$ in the extreme low-q region is compatible with cylindrical scattering objects, being the power law of the curve q^{-1}. These objects are constituted mostly of EAN and are by far denser than their environment that is made up of ACN. This organization is due to IL low affinity to acetonitrile, as it prefers to interact with itself rather than the cosolvent. The solvophobic effect is so strong that EAN *worms* are even denser than neat IL, as we said talking about the minimum in V^{M}_{EAN}.The mixtures at χ_{EAN} 0.3 and 0.5 show a similar but much less pronounced organization. Perron et al.[36] also stated that in the EAN-diluted region a strong ionic association is observed; this is consistent with our finding that when the IL is the minority compound it aggregates with itself as at χ_{EAN} 0.1. Nevertheless, it is possible to find small amounts of acetonitrile inside EAN clusters, so there are not regions containing neat IL but EAN-rich regions solvated by ACN-rich solvent. The mixtures at χ_{EAN} 0.7 and 0.9 are different. Here, EAN is the main component and it can homogeneously dissolve acetonitrile. No more component-rich regions are observed, and consequently density fluctuations disappear along with LqE. Radial distribution functions (RDFs) are widely used to understand and interpret the structure of complex systems.

Figure 10a shows how the maximum of the distance between the ammonium nitrogen and the nitrate oxygen atoms remains constant at ∼2.9 Å regardless the composition, except at χ_{EAN} 0.1 where the maximum is shifted to ∼2.8 Å. This is in line with our other findings and confirms that EAN is compressed by solvophobic effects in that mixture. The same is true for acetonitrile, but on the other side of the composition range. The RDFs computed for the centers of mass of two ACN molecules (Figure 10b) shows the first resolved peak at χ_{EAN} 0.1 at ∼4.9 Å, while at χ_{EAN} 0.9 it is found at ∼4.6 Å, once again in line with the observation on the partial molar volume. The RDFs relative to cation−acetonitrile centers of mass correlation (Figure 10c) do not show a position trend with composition; in fact, the first peak is found at ∼4.8 Å for all compositions. Nevertheless, it is interesting to observe the intensity here. For χ_{EAN} 0.1 and 0.3 mixtures (which are the systems with the most pronounced LqE), the RDFs never exceed one, meaning that a small number of molecules (i.e., less than the average bulk concentration) are in the surroundings of the cation and a solvation shell cannot properly be defined. This also means that the system is inhomogeneous on so large a scale that the "average" density is reached just for long distances, larger than the box edge. Such a heterogeneous system is better analyzed by spatial distribution functions (SDFs). The SDFs for all the simulated systems are reported in Figure S2. The cation surrounding evolves in straightforward fashion from χ_{EAN} 0.1 to

DOI: 10.1021/acs.jpclett.7b01244
J. Phys. Chem. Lett. 2017, 8, 3512−3522

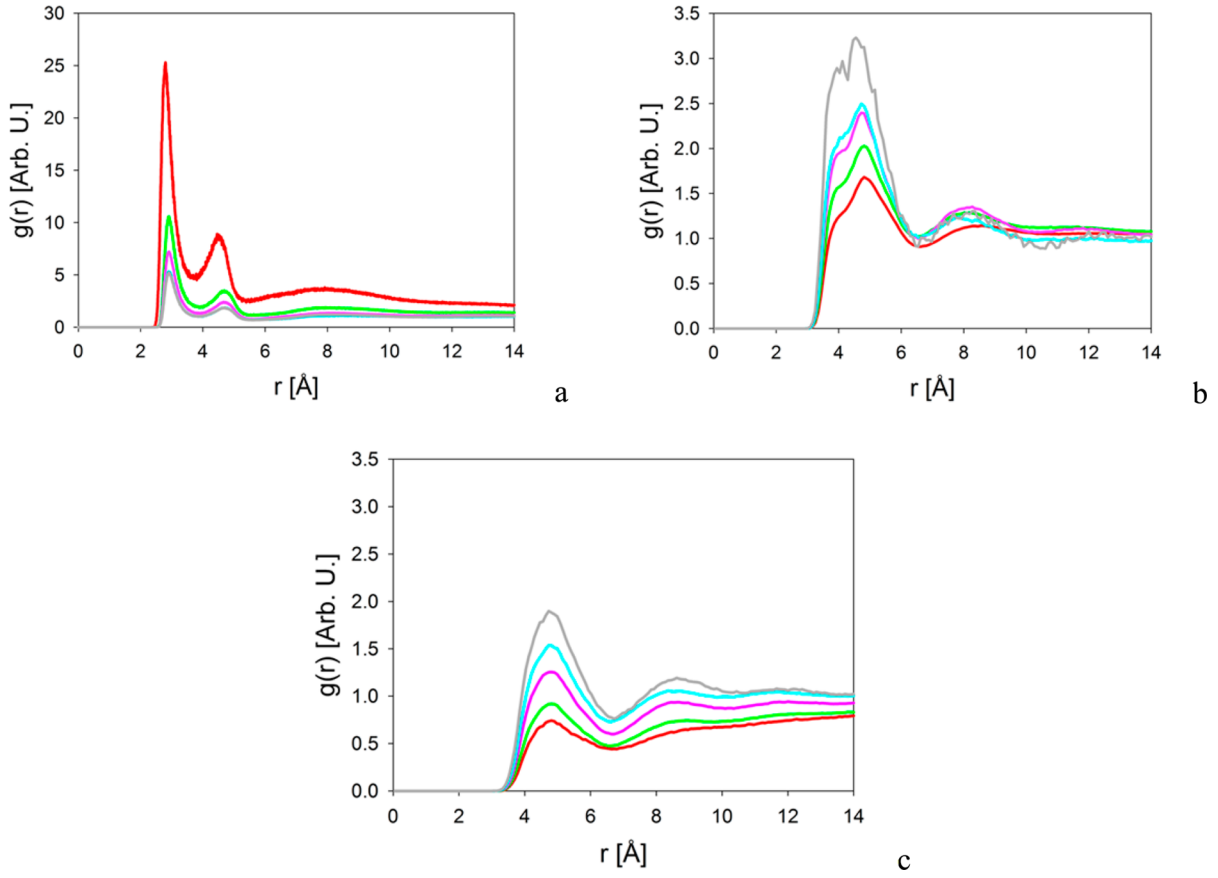

Figure 10. Radial distribution functions for the system ethylammonium nitrate−acetonitrile: (a) N_{cation}−O_{anion}; (b) COM_{ACN}−COM_{ACN}; (c) COM_{cation}−COM_{ACN}. χ_{EAN} 0.1 (red); 0.3 (green); 0.5 (purple); 0.7 (cyan); 0.9 (gray).

0.9. Acetonitrile does not compete with the nitrate to hydrogen-bond the ammonium head, but it prefers to interact with the central methylene and (less) with the terminal methyl group. The anion environment shows a clear evolving picture that complies well with all other observations. SDFs for the systems at χ_{EAN} 0.1 and 0.3 show clearly that there are absolutely no correlations between acetonitrile and nitrate, and a sharp transition is observed at χ_{EAN} 0.5 where acetonitrile starts coordinating the anion in the axial positions, competing with other anions. The acetonitrile surrounding relates nicely with the observations, in fact at χ_{EAN} 0.1, 0.3, and 0.5, the nitrate does not correlate with the acetonitrile, while the cation starts interacting with it very poorly in χ_{EAN} 0.3 mixture and more evidently at χ_{EAN} 0.5. The structural heterogeneity in χ_{EAN} 0.1, 0.3, and partially in 0.5 mixtures seems to be strongly related with the LqE in the SAXS patterns. To better understand the local structure, we performed some DFT calculations. The results are summarized as follows: First we discuss the structure of some acetonitrile clusters in order to investigate which are the intermolecular interactions governing the association in the molecular liquid. Second, we study models where one or two EAN units have been added to the acetonitrile clusters have been proposed to simulate some of the experimentally investigated mixtures and to follow how interactions between units are reciprocally affected. Ab initio calculations on acetonitrile clusters have been extensively studied by many research groups, and cluster formation is chemically very interesting.[44−46] A cluster formed by 12 acetonitrile molecules and one EAN pair was proposed as the simplest model for the ACN rich solutions (χ_{EAN} 0.1). Although the EAN self-aggregation at that composition is the main clue of this work, the proposed DFT model is a prototype for the few IL molecules solvated by acetonitrile and, perhaps more importantly, for the interface between the EAN-rich and the ACN-rich part of the system. First, we started from the acetonitrile dodecamer by optimizing its structure (see Figure 11a), then we added one ethylammonium cation and one nitrate anion (Figure 11b) with the aim of investigating if acetonitrile molecules (solvent) have a significant role in the stability of ion pairs.

Obviously, given the high number of local minima, we cannot be sure whether the localized points are describing the global minima of the potential energy surface of these complexes or local ones. The large number of possible structures is well witnessed by the fact that the structure of the dodecamer reproduced in Figure 11a has not been found to date. All the arrangements previously proposed[46] have been here studied again at B3LYP/6-311++G**, and they have been found slightly less stable. A mixing of three factors contributes to the stability of acetonitrile clusters. A first stabilizing factor is the CH−N interaction, which is present both when monomers are arranged with antiparallel orientations and when monomers form cyclic structures. Although the single interaction is very weak (the CH−N distances reproduced in Figure 11a are in fact between 2.3 and 2.8 Å), their quite high number (16) contributes to give an ordered structure to the cluster. A second stabilizing and more significant factor is the interaction between the acetonitrile dipoles, which favors the antiparallel alignment of monomers. A third factor plays a destabilizing role and arises from parallel orientation of dipoles. The contribution of each of

DOI: 10.1021/acs.jpclett.7b01244
J. Phys. Chem. Lett. 2017, 8, 3512−3522

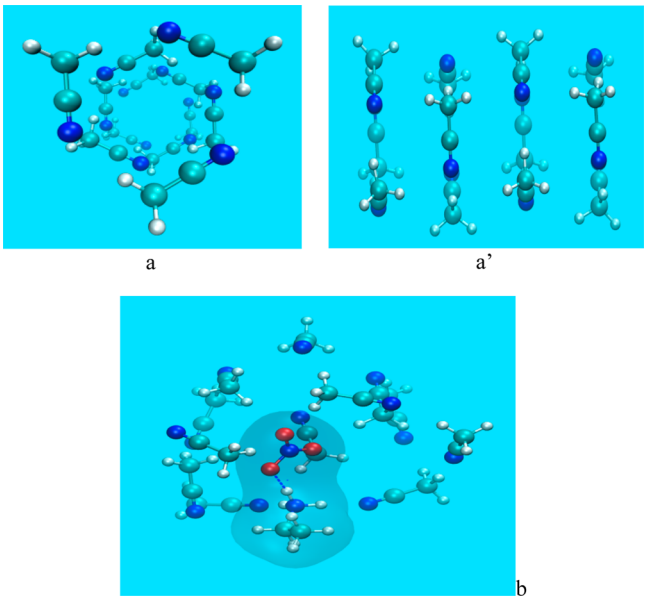

Figure 11. DFT models: (a, a′) two different views of a neat acetonitrile cluster; (b) EAN_1ACN_{12}. Ethylammonium nitrate is highlighted with shading.

these three effects has been already evaluated in several structures of acetonitrile clusters.[46] The effects of the insertion of each ionic species in the dodecamer cluster has been here evaluated by adding a single ethylammonium nitrate unit. The main result emerging from geometry optimization is that such an ion pair is stable in the acetonitrile cluster and a strong O-HN hydrogen bond (1.750 Å) connects cation and anion. In contrast, such an ion pair is not stable in the gas phase because a proton is quickly transferred from ammonium cation to nitrate anion to form the HNO_3−CH_3NH2 complex. The second important point emerging from the optimized geometry is that insertion of EAN causes a rearrangement of acetonitrile molecules. The effect of ions in acetonitrile liquid has been already investigated. In the presence of monatomic ions,[47] acetonitrile approaches the cations (Li^+, Na^+, K^+) by the side of the nitrogen atom and the anions (I^-) by the opposite side (methyl group). This means that the large dipole of the molecule aligns along the local electric field direction of the ions. In our case, two acetonitrile molecules are oriented with the N atom pointing toward the ammonium group to form two N···HN hydrogen bonds (1.919 and 1.942 Å), while arrangement of methyl groups of acetonitrile around the nitrate anion seems to be much less compact. This behavior can be attributed to the less favorable CH−O interaction that gives a very flat potential energy zone when nitrate moves around CH_3. A similar trend is found when a single ion is introduced into the dodecamer acetonitrile: in the $(NO_3^-)(CH_3CN)_{12}$ (Figure 12a) complex, nitrogen of acetonitrile points away from nitrate, whereas in the $(CH_2NH_3^+)(CH_3CN)_{12}$ (Figure 12b) complex, the coordination of nitrogen atoms around the ammonium group is driven by the formation of three NH−N hydrogen bonds. From this simple model, it emerges that the presence of EAN has two important effects which can change deeply the structure of acetonitrile liquid: introduction of electrostatic charges gives rise to Coulombic forces which drive the orientation of acetonitrile dipoles, and the ammonium group allows the formation of NH-N hydrogen bonding with acetonitrile. Both effects are absent in neat acetonitrile.

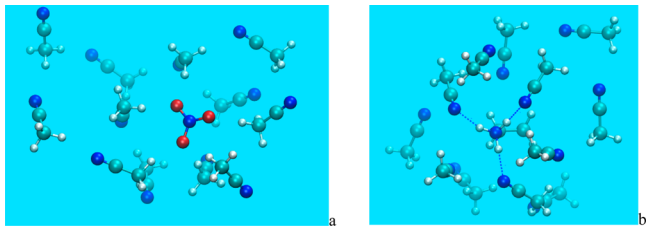

Figure 12. DFT models: (a) $(NO_3^-)(CH_3CN)_{12}$ cluster and (b) $(CH_2NH_3^+)(CH_3CN)_{12}$ cluster.

To simulate solutions at higher concentration of EAN and describe the simultaneous presence of more ion pairs, a larger model was proposed where two EAN units have been added to 18 acetonitrile molecules starting from an arrangement where each EAN pair is separated by acetonitrile molecules. Such structure has been studied again at the B3LYP/6-311++G** level, and its optimized geometry is reproduced in Figure 13.

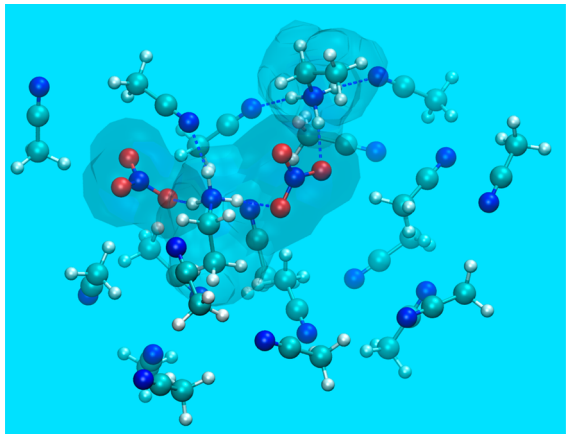

Figure 13. DFT model of EAN_2ACN_{18}. Ethylammonium nitrate is highlighted with shading.

We observe that cation and anion continue to be connected by a strong hydrogen bond 1.777 and 1.686 Å and that ,as for the smaller model, two acetonitrile molecules are coordinated around each ethylammonium cation though NH−N hydrogen bonds (1.928 and 1.928 Å and 2.064 and 2.123 Å). Because two ion pairs do not approach each other but remain separated by a layer of acetonitrile molecules, we can assert that the favorable interactions between acetonitrile and cations are one of the factors that hinders the self-association of ionic components in solutions.

Self-aggregation of EAN in acetonitrile has been further evaluated by a second model where cations and anions were initially oriented to form a cyclic structure with an alternation between ethylammonium and nitrate ions as expected for two ion pairs in the gas phase (see Figure 14a). Such tetrameric structure was introduced in the same cluster of 18 acetonitrile molecules, and its geometry was studied at the same level of the first model. The optimized geometry (Figure 14b) maintains the ionic alternation of the initial structure; however, the formation of NH−N interactions between acetonitrile and cationic polar head of ethylammonium opens the ionic cyclic structure. In addition, the stability of such a second model is comparable with that in which ion pairs are completely separated by acetonitrile molecules.

DOI: 10.1021/acs.jpclett.7b01244
J. Phys. Chem. Lett. 2017, 8, 3512−3522

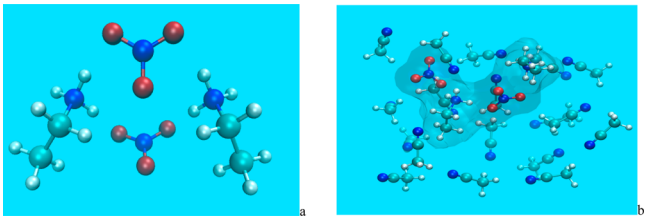

Figure 14. DFT models: (a) EAN_2 and (b) EAN_2ACN_{18}. Ethylammonium nitrate is highlighted with shading.

In summary, we probed the structure in the whole composition range of the binary mixtures EAN−acetonitrile using volumetric measures, small-angle X-ray scattering, classical molecular dynamics, and DFT calculations. Our results suggest a strong inhomogeneity in the mixtures where EAN is the minority compound. This is stated by an intense feature in the extreme low-q region of the SAXS pattern and by the minima in the partial molar volumes. This behavior was already observed for other EAN-containing mixtures, but this is the first work which quantify the density fluctuations associated with the LqE. Moreover, our MD simulations enable us to say that the physical objects responsible for the density fluctuations are wormlike EAN structures, which are denser than the neat IL. Regarding DFT calculations, although we are well aware of the spatial limits of the molecular aggregates considered, it is quite clear that EAN and acetonitrile have an outstanding reciprocal effect: on one hand, ions of EAN orient the dipolar acetonitrile molecules, and on the other side, acetonitrile effectively interacts with the cations preventing self-association of EAN and allowing the solubility of the two components.

EXPERIMENTAL SECTION

Ethylammonium nitrate was purchased at IoLiTec (>98%) and was pumped in high vacuum under slight warming at 50 °C overnight to remove residual water. The final content of water was checked with 1H NMR, and it was undetectable (<0.005%). Acetonitrile anhydrous was purchased at Sigma-Aldrich (99.8%) and used without further treating. All the samples were prepared by weighing in controlled atmosphere of dry argon. SWAXS patterns were collected at the ID02 beamline (ESRF-Grenoble). SAXS (q range 0.008−0.683 $Å^{-1}$) and WAXS patterns (0.565−4.280 $Å^{-1}$) were collected simultaneously setting the sample at 1 m from the SAXS detector and using the overlapping q region to check data consistency. Mixtures were injected into a flow-through thermostated quartz capillary with a 2 mm o.d. The capillary was carefully washed with Milli-Q water and ethanol before each sample was injected. All the measurements were taken at least five times at 25 °C and then averaged to reduce noise effects. The raw data were treated by just subtracting the cell contribution. The WAXS patterns in the Supporting Information were collected in a 2 mm o.d. quartz capillary at room temperature and pressure using the diffractometer developed by Prof. Ruggero Caminiti, located in the Department of Chemistry of "La Sapienza" University of Rome (Italian Patent No. 01126484-23 June, 1993).[48] Details on how the data were treated can be found in ref 47. Density measurements were collected using an Anton Paar DMA 4500 M vibrating tube densimeter (PSCM-Grenoble).

COMPUTATIONAL DETAILS

The simulations were carried out using AMBER14[49] with GAFF[50] force field. The atomic charges for EAN were computed at the B3LYP/aug-cc-pVTZ level of theory using Gaussian09d[51] and RESP[52] algorithm. All the simulation boxes were prepared using PACKMOL[53] to obtain an initial random distribution of the molecules. The numbers of each molecule were chosen to obtain the same molar fraction of the respective experimental sample (details in Table S3). A multiplicative dielectric constant of 1.8 was set within the box containing EAN; this is equivalent to rescale the punctual charges with a factor ∼0.75, and we have shown how this procedure enhances the results when protic ILs are involved.[54] The simulations consisted of 10^7 minimization cycles, a short (500 ps) *NVT* phase to heat the system from 0 to 50 K, a *NPT* equilibration phase (20 ns) at 300 K to adjust the density and avoid holes in the structure, a *NVT* equilibration phase (20 ns) at 300 K, and a *NVT* productive phase (10 ns) at 300 K. A time step of 2 fs was used for each passage, and SHAKE algorithm was active to constrain heavy atom−hydrogen distances. All the results shown are computed only on the last *NVT* phase. The structure factor from the simulations was obtained following our standard procedure.[48] RDFs and SDFs were computed using the TRAVIS[55] software. DFT calculations were performed using Gaussian 09d at the B3LYP/6-311++G** level of theory.

ASSOCIATED CONTENT

Supporting Information

The Supporting Information is available free of charge on the ACS Publications website at DOI: 10.1021/acs.jpclett.7b01244.

Volumetric properties for all the mixtures discussed in this work; comparison between computed and experimental densities and WAXS patterns; fitting parameters for excess volume values; spatial distribution functions obtained from the simulations; number of molecules in each molecular dynamics simulation box (PDF)

AUTHOR INFORMATION

Corresponding Authors

*E-mail: alessandro.mariani@esrf.fr.

*E-mail: lorenzo.gontrani@uniroma1.it.

ORCID

Alessandro Mariani: 0000-0002-3686-2169

Lorenzo Gontrani: 0000-0001-8212-7029

Present Address

⊥A.M.: European Synchrotron Radiation Facility, 71 Avenue des Martyrs, 38000 Grenoble, France.

Notes

The authors declare no competing financial interest.

ACKNOWLEDGMENTS

For this work, we thank the European Synchrotron Radiation Facility (ESRF-Grenoble, France) for granting us beam time in the context of the SC-4272 experiment "Exploring structural changes in Protic Ionic Liquids mixtures upon the co-solvent polarity". We also gratefully thank Dr. Diego Pontoni and Dr. Pierre Lloria for their efforts and for allowing us to use PSCM instrumentation. We also acknowledge Prof. Enrico Bodo for insightful conversations. The small- and wide-angle scattering experiments were performed on beamline ID02 at ESRF.

DOI: 10.1021/acs.jpclett.7b01244
J. Phys. Chem. Lett. 2017, 8, 3512−3522

REFERENCES

(1) Marsh, K. N.; Boxall, J. A.; Lichtenthaler, R. Room Temperature Ionic Liquids and Their Mixtures—a Review. *Fluid Phase Equilib.* **2004**, *219* (1), 93−98.

(2) Canongia Lopes, J. N.; Costa Gomes, M. F.; Husson, P.; Pádua, A. A. H.; Rebelo, L. P. N.; Sarraute, S.; Tariq, M. Polarity, Viscosity, and Ionic Conductivity of Liquid Mixtures Containing [C 4 C 1 im][Ntf 2] and a Molecular Component. *J. Phys. Chem. B* **2011**, *115* (19), 6088−6099.

(3) Docampo-Álvarez, B.; Gómez-González, V.; Méndez-Morales, T.; Carrete, J.; Rodríguez, J. R.; Cabeza, Ó.; Gallego, L. J.; Varela, L. M. Mixtures of Protic Ionic Liquids and Molecular Cosolvents: A Molecular Dynamics Simulation. *J. Chem. Phys.* **2014**, *140* (21), 214502.

(4) Oleinikova, A.; Bonetti, M. Critical Behavior of the Electrical Conductivity of Concentrated Electrolytes: Ethylammonium Nitrate in N-Octanol Binary Mixture. *J. Solution Chem.* **2002**, *31* (5), 397−413.

(5) Chagnes, A.; Tougui, A.; Carré, B.; Ranganathan, N.; Lemordant, D. Abnormal Temperature Dependence of the Viscosity of Ethylammonium Nitrate−Methanol Ionic Mixtures. *J. Solution Chem.* **2004**, *33* (3), 247−255.

(6) Atkin, R.; Warr, G. G. Phase Behavior and Microstructure of Microemulsions with a Room-Temperature Ionic Liquid as the Polar Phase. *J. Phys. Chem. B* **2007**, *111* (31), 9309−9316.

(7) Kanzaki, R.; Uchida, K.; Song, X.; Umebayashi, Y.; Ishiguro, S. Acidity and Basicity of Aqueous Mixtures of a Protic Ionic Liquid, Ethylammonium Nitrate. *Anal. Sci.* **2008**, *24* (10), 1347−1349.

(8) Atkin, R.; Warr, G. G. The Smallest Amphiphiles: Nanostructure in Protic Room-Temperature Ionic Liquids with Short Alkyl Groups. *J. Phys. Chem. B* **2008**, *112* (14), 4164−4166.

(9) Litaeim, Y.; Dhahbi, M. Measurements and Correlation of Viscosity and Conductivity for the Mixtures of Ethylammonium Nitrate with Organic Solvents. *J. Mol. Liq.* **2010**, *155* (1), 42−50.

(10) Zarrougui, R.; Dhahbi, M.; Lemordant, D. Volumetric Properties of Ethylammonium Nitrate + γ-Butyrolactone Binary Systems: Solvation Phenomena from Density and Raman Spectroscopy. *J. Solution Chem.* **2010**, *39* (10), 1531−1548.

(11) Shi, L.; Zhao, M.; Zheng, L. Micelle Formation by N-Alkyl-N-Methylpyrrolidinium Bromide in Ethylammonium Nitrate. *Colloids Surf., A* **2011**, *392* (1), 305−312.

(12) Greaves, T. L.; Kennedy, D. F.; Kirby, N.; Drummond, C. J. Nanostructure Changes in Protic Ionic Liquids (PILs) through Adding Solutes and Mixing PILs. *Phys. Chem. Chem. Phys.* **2011**, *13* (30), 13501.

(13) Smith, J. A.; Webber, G. B.; Warr, G. G.; Atkin, R. Rheology of Protic Ionic Liquids and Their Mixtures. *J. Phys. Chem. B* **2013**, *117* (44), 13930−13935.

(14) Mariani, A.; Russina, O.; Caminiti, R.; Triolo, A. Structural Organization in a Methanol:ethylammonium Nitrate (1:4) Mixture: A Joint X-ray/Neutron Diffraction and Computational Study. *J. Mol. Liq.* **2015**, *212*, 947−956.

(15) Russina, O.; Macchiagodena, M.; Kirchner, B.; Mariani, A.; Aoun, B.; Russina, M.; Caminiti, R.; Triolo, A. Association in Ethylammonium Nitrate−dimethyl Sulfoxide Mixtures: First Structural and Dynamical Evidences. *J. Non-Cryst. Solids* **2015**, *407*, 333−338.

(16) Canongia Lopes, J. N.; Esperança, J. M. S. S.; de Ferro, A. M.; Pereiro, A. B.; Plechkova, N. V.; Rebelo, L. P. N.; Seddon, K. R.; Vázquez-Fernández, I. Protonic Ammonium Nitrate Ionic Liquids and Their Mixtures: Insights into Their Thermophysical Behavior. *J. Phys. Chem. B* **2016**, *120* (9), 2397−2406.

(17) Schroer, W.; Triolo, A.; Russina, O. Nature of Mesoscopic Organization in Protic Ionic Liquid−Alcohol Mixtures. *J. Phys. Chem. B* **2016**, *120* (9), 2638−2643.

(18) Mariani, A.; Dattani, R.; Caminiti, R.; Gontrani, L. Nanoscale Density Fluctuations in Ionic Liquid Binary Mixtures with Non-amphiphilic Compounds: First Experimental Evidence. *J. Phys. Chem. B* **2016**, *120* (40), 10540−10546.

(19) Mariani, A.; Campetella, M.; Fasolato, C.; Daniele, M.; Capitani, F.; Bencivenni, L.; Postorino, P.; Lupi, S.; Caminiti, R.; Gontrani, L. A Joint Experimental and Computational Study on Ethylammonium Nitrate-Ethylene Glycol 1:1 Mixture. Structural, Kinetic, Dynamic and Spectroscopic Properties. *J. Mol. Liq.* **2017**, *226*, 2−8.

(20) Hayes, R.; Imberti, S.; Warr, G. G.; Atkin, R. Amphiphilicity Determines Nanostructure in Protic Ionic Liquids. *Phys. Chem. Chem. Phys.* **2011**, *13* (8), 3237−3247.

(21) Hayes, R.; Imberti, S.; Warr, G. G.; Atkin, R. Pronounced Sponge-like Nanostructure in Propylammonium Nitrate. *Phys. Chem. Chem. Phys.* **2011**, *13* (30), 13544.

(22) Triolo, A.; Russina, O.; Bleif, H.-J.; Di Cola, E. Nanoscale Segregation in Room Temperature Ionic Liquids †. *J. Phys. Chem. B* **2007**, *111* (18), 4641−4644.

(23) Russina, O.; Triolo, A.; Gontrani, L.; Caminiti, R. Mesoscopic Structural Heterogeneities in Room-Temperature Ionic Liquids. *J. Phys. Chem. Lett.* **2012**, *3* (1), 27−33.

(24) Russina, O.; Sferrazza, A.; Caminiti, R.; Triolo, A. Amphiphile Meets Amphiphile: Beyond the Polar−Apolar Dualism in Ionic Liquid/Alcohol Mixtures. *J. Phys. Chem. Lett.* **2014**, *5* (10), 1738−1742.

(25) Jiang, H. J.; FitzGerald, P. A.; Dolan, A.; Atkin, R.; Warr, G. G. Amphiphilic Self-Assembly of Alkanols in Protic Ionic Liquids. *J. Phys. Chem. B* **2014**, *118* (33), 9983−9990.

(26) Greaves, T. L.; Drummond, C. J. Ionic Liquids as Amphiphile Self-Assembly Media. *Chem. Soc. Rev.* **2008**, *37* (8), 1709.

(27) Wu, X.; Liu, Z.; Huang, S.; Wang, W. Molecular Dynamics Simulation of Room-Temperature Ionic Liquid Mixture of [bmim]-[BF4] and Acetonitrile by a Refined Force Field. *Phys. Chem. Chem. Phys.* **2005**, *7* (14), 2771.

(28) Jiang, W.; Wang, Y.; Voth, G. A. Molecular Dynamics Simulation of Nanostructural Organization in Ionic Liquid/Water Mixtures †. *J. Phys. Chem. B* **2007**, *111* (18), 4812−4818.

(29) Nishikawa, K.; Kasahara, Y.; Ichioka, T. Inhomogeneity of Mixing in Acetonitrile Aqueous Solution Studied by Small-Angle X-Ray Scattering. *J. Phys. Chem. B* **2002**, *106* (3), 693−700.

(30) Tee, E. M.; Awichi, A.; Zhao, W. Probing Microstructure of Acetonitrile−Water Mixtures by Using Two-Dimensional Infrared Correlation Spectroscopy. *J. Phys. Chem. A* **2002**, *106* (29), 6714−6719.

(31) Bakó, I.; Megyes, T.; Pálinkás, G. Structural Investigation of Water−acetonitrile Mixtures: An Ab Initio, Molecular Dynamics and X-Ray Diffraction Study. *Chem. Phys.* **2005**, *316* (1−3), 235−244.

(32) Huang, N.; Nordlund, D.; Huang, C.; Bergmann, U.; Weiss, T. M.; Pettersson, L. G. M.; Nilsson, A. X-Ray Raman Scattering Provides Evidence for Interfacial Acetonitrile-Water Dipole Interactions in Aqueous Solutions. *J. Chem. Phys.* **2011**, *135* (16), 164509.

(33) Chen, J.; Sit, P. H.-L. Ab Initio Study of the Structural Properties of Acetonitrile−water Mixtures. *Chem. Phys.* **2015**, *457*, 87−97.

(34) Newman, K. E. Kirkwood−Buff Solution Theory: Derivation and Applications. *Chem. Soc. Rev.* **1994**, *23* (1), 31−40.

(35) Nikolova, P. V.; Duff, S. J. B.; Westh, P.; Haynes, C. A.; Kasahara, Y.; Nishikawa, K.; Koga, Y. A Thermodynamic Study of Aqueous Acetonitrile: Excess Chemical Potentials, Partial Molar Enthalpies, Entropies and Volumes, and Fluctuations. *Can. J. Chem.* **2000**, *78* (12), 1553−1560.

(36) Perron, G.; Hardy, A.; Justice, J.-C.; Desnoyers, J. E. Model System for Concentrated Electrolyte Solutions: Thermodynamic and Transport Properties of Ethylammonium Nitrate in Acetonitrile and in Water. *J. Solution Chem.* **1993**, *22* (12), 1159−1178.

(37) Grant-Taylor, D. F.; Macdonald, D. D. Thermal Pressure and Energy−volume Coefficients for the Acetonitrile + Water System. *Can. J. Chem.* **1976**, *54* (17), 2813−2819.

(38) Redlich, O.; Kister, A. T. Algebraic Representation of Thermodynamic Properties and the Classification of Solutions. *Ind. Eng. Chem.* **1948**, *40* (2), 345−348.

(39) Dixit, S.; Crain, J.; Poon, W. C. K.; Finney, J. L.; Soper, A. K. Molecular Segregation Observed in a Concentrated Alcohol−water Solution. *Nature* **2002**, *416* (6883), 829−832.

DOI: 10.1021/acs.jpclett.7b01244
J. Phys. Chem. Lett. 2017, 8, 3512−3522

(40) Hayes, R.; Imberti, S.; Warr, G. G.; Atkin, R. How Water Dissolves in Protic Ionic Liquids. *Angew. Chem., Int. Ed.* **2012**, *51* (30), 7468−7471.
(41) Saleh, M. a.; Akhtar, S.; Ahmed, M. S.; Uddin, M. H. Excess Molar Volumes and Thermal Expansivities of Aqueous Solutions of Dimethylsulfoxide, Tetrahydrofuran and 1,4-Dioxane. *Phys. Chem. Liq.* **2002**, *40* (5), 621−635.
(42) Navia, P.; Troncoso, J.; Romaní, L. Viscosities for Ionic Liquid Binary Mixtures with a Common Ion. *J. Solution Chem.* **2008**, *37* (5), 677−688.
(43) Bhatia, A. B.; Thornton, D. E. Structural Aspects of the Electrical Resistivity of Binary Alloys. *Phys. Rev. B* **1970**, *2* (8), 3004−3012.
(44) Nigam, S.; Majumder, C. Growth Pattern and Electronic Properties of Acetonitrile Clusters: A Density Functional Study. *J. Chem. Phys.* **2008**, *128* (21), 214307.
(45) Mata, R. A.; Costa Cabral, B. J. Structural, Energetic, and Electronic Properties of (CH3CN)2−8 Clusters by Density Functional Theory. *J. Mol. Struct.: THEOCHEM* **2004**, *673* (1−3), 155−164.
(46) Remya, K.; Suresh, C. H. Cooperativity and Cluster Growth Patterns in Acetonitrile: A DFT Study. *J. Comput. Chem.* **2014**, *35* (12), 910−922.
(47) Albertí, M.; Amat, A.; De Angelis, F.; Pirani, F. A Model Potential for Acetonitrile: From Small Clusters to Liquid. *J. Phys. Chem. B* **2013**, *117* (23), 7065−7076.
(48) Caminiti, R.; Albertini, V. R. The Kinetics of Phase Transitions Observed by Energy-Dispersive X-Ray Diffraction. *Int. Rev. Phys. Chem.* **1999**, *18* (2), 263−299.
(49) Case, D. a; Cheatham, T. E.; Darden, T.; Gohlke, H.; Luo, R.; Merz, K. M.; Onufriev, A.; Simmerling, C.; Wang, B.; Woods, R. J. The Amber Biomolecular Simulation Programs. *J. Comput. Chem.* **2005**, *26* (16), 1668−1688.
(50) Wang, J.; Wolf, R. M.; Caldwell, J. W.; Kollman, P. A.; Case, D. A. Development and Testing of a General Amber Force Field. *J. Comput. Chem.* **2004**, *25* (9), 1157−1174.
(51) Frisch, M. J.; Trucks, G. W.; Schlegel, H. B.; Scuseria, G. E.; Robb, M. A.; Cheeseman, J. R.; Scalmani, G.; Barone, V.; Mennucci, B.; Petersson, G. A.; et al. *Gaussian 09*, revision D.01; Gaussian, Inc.: Wallingford, CT, 2009.
(52) Dupradeau, F.-Y.; Pigache, A.; Zaffran, T.; Savineau, C.; Lelong, R.; Grivel, N.; Lelong, D.; Rosanski, W.; Cieplak, P. The R.E.D. Tools: Advances in RESP and ESP Charge Derivation and Force Field Library Building. *Phys. Chem. Chem. Phys.* **2010**, *12* (28), 7821.
(53) Martínez, L.; Andrade, R.; Birgin, E. G.; Martínez, J. M. PACKMOL: A Package for Building Initial Configurations for Molecular Dynamics Simulations. *J. Comput. Chem.* **2009**, *30* (13), 2157−2164.
(54) Mariani, A.; Caminiti, R.; Campetella, M.; Gontrani, L. Pressure-Induced Mesoscopic Disorder in Protic Ionic Liquids: First Computational Study. *Phys. Chem. Chem. Phys.* **2016**, *18* (4), 2297−2302.
(55) Brehm, M.; Kirchner, B. TRAVIS - A Free Analyzer and Visualizer for Monte Carlo and Molecular Dynamics Trajectories. *J. Chem. Inf. Model.* **2011**, *51* (8), 2007−2023.

DOI: 10.1021/acs.jpclett.7b01244
J. Phys. Chem. Lett. 2017, 8, 3512−3522